

*Full Length Research Paper*

# **Error concealment innovator based on the multi-directional interpolation by using the similarity segmentation**

**Alaa Kh. Al-Azzawi<sup>1\*</sup>, M. Iqbal Saripan<sup>2</sup>, Adznan Jantan<sup>2</sup> and Rahmita Wirza O. K. Rahmat<sup>3</sup>**

<sup>1</sup>Department of Computer and Communication Engineering, Faculty of Engineering, UPM, A-10-17 South City, Seri Kembangan, Serdang 43300, Selangor-Malaysia.

<sup>2</sup>Department of Computer and Communication Engineering, Faculty of Engineering, University Putra Malaysia.

<sup>3</sup>Department of Multimedia, Faculty of Computer Science and Information Technology, University Putra Malaysia.

Accepted 6 December, 2010

**In this paper, an error concealment algorithm based on the multi-directional interpolation (MDI) was proposed. The algorithm has the capability to recover the damaged blocs, whether located in smooth or non-smooth areas. In the case of smooth regions, the missing coefficients were estimated by interpolating these coefficients with undamaged adjacent pixels. While, in the non-smooth areas (for example edge components), these blocks were portioned to at least four quarters, in the intention to exploit all border pixels. In the meantime, pixels of the border left and right were estimated with horizontal interpolation, pixels of the border top, and bottom were estimated with vertical interpolation, Whereas the remaining pixels of each quarter were simultaneously guessed with vertical and horizontal interpolation. Finally, another algorithm to convert pixels to feet proposed. The motivation behind the current implementation and the problem that we aim to solve lies on how to convert the size of the base and height of triangles from pixels-to-feet. In the intention to calculate the areas of these triangles, for the purpose of compensation. The experimental results showed that the number of pixels occurred and the error was relatively low.**

**Key words:** Error Concealment (EC), Multi-Directional Interpolation (MDI), image segmentation, edge detection.

## **INTRODUCTION**

Error Concealment (EC) is a post-processing technique that has been researched so that a close approximation of the original signal from the decoder can be obtained by exploiting the correctly received information. Numerous techniques have been developed to face this problem. Chi et al. (2005), explained that parts of bit streams may be corrupted by noise over the wireless communication networks with error-prone channels, and some packets may be lost over the bandwidth limited networks when congestion happens. These situations would make the visual quality of the reconstructed video seriously degraded at the receiver side if no post-processing techniques are adopted. In recent years, some wavelet-based coders Kim et al. (2000) used each of the FEC

methods and multiple correlated bit-streams to transmit and decode each bit-stream independently, which provide additional error resilience at high loss rates Kim et al. (2004).

The decoder, furthermore, applies a post-processing concealment procedure to the received bit-streams to conceal packets that cannot be recovered by using FEC and multiple bit-streams solely. Because of using the predictive coding and Variable Length Coding (VLC) in video compression Y. Wang et al. (2000), the trend will be confined to the applications of the passive concealment techniques to avoid network congestion and to reduce data transmission. The passive concealment does not result in perfect reconstruction of damaged blocks, but does not require any extra data, whereas active concealment transmits extra data at the decoder. Therefore, while this technique increases network congestion, it permits perfect reconstruction. The typical

\*Corresponding author. E-mail: [ali\\_ksaleh2010@yahoo.com](mailto:ali_ksaleh2010@yahoo.com).

passive concealment techniques were proposed by Hemami and Meng (1995) and Shin et al. (1999). In general, those proposed techniques interpolate each damaged pixel in an error block from its corresponding pixel in the four neighboring blocks.

In general, the discrete cosine transforms (DCT) is employed to transform time domain signals to frequency domain coefficients so that signal energies are concentrated in low frequency areas. Then, those frequency components can be effectively encoded with quantization and entropy encoding methods. Variable Length Coding (VLC) is further adopted to remove the statistical redundancy, where much more coefficients are zeros after quantization (Guo et al., 2009). The method in Lee et al. (2003) is a contour for coding the DCT-based image compression that supposed to prevent errors from propagating across the block boundary with an acceptable overhead. The method described in Tsekeridou and Pitas, (2000) is a spatial split-match EC method, which attempts to spatially match the top and bottom neighboring regions and conceal the region in the direction of the match. For clarification, in the case where the content of the local image has low details, this leads to the appearance of some unwanted effects (that is blurring and blockiness).

In this paper, we need to apportion the damaged blocks into multi-geometric insets with the intention to facilitate the separation of both smooth and non-smooth areas with each other. In this proposal, and during the process of portioning, the attention was focused on how to create triangles from both damaged and undamaged areas for the purpose of compensation. The motivation behind the current implementation and the problem that the study intends to solve, lies on how to convert the lengths of each base and height of the triangles from pixels-to-feet in the intention to calculate the area of each truncated triangle for the purpose of concealment. As a result, this had greatly facilitated to extract both vertical and horizontal image gradients. In most cases, the image gradients were efficiently carried out either, by enlarging the target region to select the suited interpolation process, in which a professional restoration for concealing these patches with minimal deformation is needed, or by applying the mask operators.

### Earlier work

Error concealment, are pragmatism uses for redeeming or assessing a data loss due to the transmission errors. Many of the proposed EC methods used the correlation process between the damaged blocks and undamaged adjacent blocks. Error concealment methods can be classified into three categories: 1) spatial error concealment, 2) temporal error concealment, and 3) spatial-temporal based error concealment. One of the most common aspects found in the spatial continuities

was the proper usage of Markov processes. Markov processes are very beneficial in the statistical image forming an image manipulating implementation (Simchony et al., 1990). This might belong to their nature on local dependence. Moreover, the digital images contained a tremendous number of pixels, which can be utilized in so many applications as a problem solution, such as edge detection and image compression.

In Kaup et al. (2005), another efficient scheme was applied to spatial error concealment, in which a 2D-DFT basis function for approximating surrounding error-free received image samples is achieved. Here, the area that corresponds to the lost macro-block is copied to the lost image area. Whereas, the method proposed in Hsia (2004), presents an efficient spatial interpolation process to reconstruct the corrupted image, and also to achieve special well-done quality for substantive image edges. In temporal EC methods, estimation of loss motion vectors MV's to the corrupted MB's is achieved according to the temporal redundant information (Suh and Ho, 2004). Al-Mualla et al. (1999) proposed an approach to the temporal error concealment based on both bilinear motion field interpolation and boundary matching scheme. On the other hand, Zeng and Liu (1999) presented an MDI contour as one of the geometric structure schemes for such a problem Zeng and Liu (1999).

Recently, several EC methods have been developed and employed, such as forward error correction FEC (Nafaa et al., 2008), layered coding (Fu et al., 2005), and multiple descriptions coding MDC (Wang et al., 2005). We found that the model proposed by Bajic (2006) is well known, and gives slightly better results than that in bilinear interpolation method proposed by Al-Mualla et al. (1999). The method in Tsekeridou and Pitas (2000), describes a new approach to the spatial split-match EC for concealing loss blocks, which attempts to spatially match top and bottom neighboring regions, and also conceals the region in the direction of the match. The conventional method lacks not only for producing artifacts but also edge discontinuities, if the content of the local image has low details. Kung et al. (2006), proposed a spatial and temporal EC technique for video transmission over noisy channels. Summarizing, this scheme is more efficient than the previous methods. First, spatial EC contour uses to compensate the lost blocks within intra-coded frames, in which no meaningful temporal information is available. Secondly, a dynamic mode-weighted EC method utilizes for replenishing missing pixels within the lost macro-block of inter-coded frames. For clarity, if neighboring incorrect macro-blocks were recovered within big-matching errors, this will do harm to reconstruct the next ones. To overcome the drags of the recovery dependency problems, Chen et al. (2005) proposed using the repetitive boundaries to assess the filling-in process.

On the other hand, Chung et al. (2007), proposed a

mongrel error concealment MEC algorithm based-on the 8-neighboring from the corrupted MBs. They classified the corrupted MBs into three sorts: 1) high variance sort HVS, 2) low variance sort LVS, and 3) dominance sort DS. Moreover, the proposed MEC method can easily be determining what kind of EC method should be utilized to recover the damaged MB. To date, there have been only a few processors related to the impact of the blurring resulting from the edge detection process, in which secondary-order derivative is achieved. Rombaut et al. (2009), suggested an adaptive EC method for both low and high-frequencies coefficients based on a heterogeneous Gaussian Markov random field model GMRF. On the other hand, novel concepts for boundary matching, such as multiple frames of still images (Lee et al., 2001) used to match the boundaries, which utilize the boundary fleecy property in the decoded and succeeding frames, and also the best matching block (Feng et al., 1997) used to modify the boundary matching process to assess the best matching block in the reference frame for recovering the corrupted MB have been considered. An interpolation scheme is commonly used as an empirical model which is developed to interpolate the pixel values in the error blocks EB, by using the pixels within the adjacent matchable blocks is suggested in Li and Orchard (2002). This method does not provide a perfect solution to non-smooth areas. Wang et al. (1998) proposed new spatial EC approach towards neighborhood matchable error concealment (NMEC) based-on a priori information block wise similarity within the image to be filled. Li et al. (2002) discuss how image data in the corrupted patches can be recovered in a sequential style, so that efficient reconstruction can be achieved with the successfully received pixels, and also on the previously recovered ones.

The following approaches applying both the biased anisotropic diffusion contour and the total variation as an alternative to the first had been proposed (Yang and Hu, 1997; Gothandaraman et al., 2001). Similar approach to the previous methods has been suggested in Alter F, et al. (2004). This new method uses a weight total variation to minimize the impact of the blurring.

Keeping in mind that we want to avoid both the blurring and the blocking influence for those proposed methods. For clarity, these influences have been formulated into energy minimization problems. Rongfu et al. (2004) proposed a content adaptive error concealment technique, in which edge information extracted from the surrounding blocks is used. Here, the EB is classified into three categories: 1) uniform block, 2) edge block, and 3) texture block.

There is another pair of approaches of two errors pliable coding lay-outs: 1) wavelet-based image transmission based on the data involved, and genetic algorithms GA's and proposed by Kang and Leou (2006).

In this scenario, JPEG-2000 images must be analyzed into six wavelet levels (levels 0 to 5). At the transmitting

side, for levels 0 to 2, some meaningful data serviceable for EC performed at the decoder is elicited and guarantees to the compressed image bit-stream. At the receiving side, the meaningful data for each corrupted code block is elicited and utilized to facilitate error concealment, whereas, for levels 3 to 5. The coefficients of each corrupted code block are replaced by zeros. To achieve more image coefficients, super-resolution methods are utilized to process image sequences for the purpose of obtaining still images as well as improving resolution. The method suggested in Wang et al. (2010), is an example to the image super resolution SR approach based on discovering the sparse association between input image patches and a large example image patch set.

The determination order of an adaptive error concealment AEC for the EB within a connected region has been proposed in Qian et al. (2009). The AEC for the macro-blocks is determined according to the external macro-blocks pattern information rather than the conventional raster scan mode. The method proposed by Persson et al. (2008) is a Gaussian mixture model GMM. This method used to improve the peak signal-to-noise ratio compared to the rest of the other traditional methods. Moreover, it is asymptotically optimal, in the case where the number of mixture components goes to infinity. Here is another similar hybrid-EC technique, where a mixture-based estimator and least squared technique are used to solve the problems of the spatio-temporal error concealment (STEC) have been proposed in Persson and Eriksson (2009). To compare the STEC technique with the GMM technique, the new technique is be based on more surrounding pixels to the lost block, while maintaining a low computational complexity. Below is another suggested technique for EC, in which PDE-based algorithm used to refine the reconstruction process, for reducing the blocking influence, and also well-preserve for the reference structure of macro-block (Chen et al., 2008).

The work in Ma et al. (2008), concerned with multiple descriptions coding (MDC), and also known as dispersive packetization. Here, the MDC divides the video stream into equally multiple streams, which are sending to the destination through different channels. Moreover, an innovator of multi-hypothesis error concealment (MHC) was suggested, in which a number of the video frames after the loss, are error-concealing instead of decoding directly. In fact, simultaneous temporal-interpolation used in improving the reconstructed video quality in Park et al. (2009), can be introduced as an error tracking model, to estimate both the concealment and propagation errors of EC method using this model.

## MATERIALS AND METHODS

### Proposed method

Figure 1 shows the MDI proposed interpolation innovator. Where,  $P_{VT}$ ,  $P_{VB}$ ,  $P_{HL}$ , and  $P_{HR}$ , are the vertical top, vertical bottom, horizontal left, and horizontal right adjacent pixels, respectively. In this paper, the interpolation process achieved so

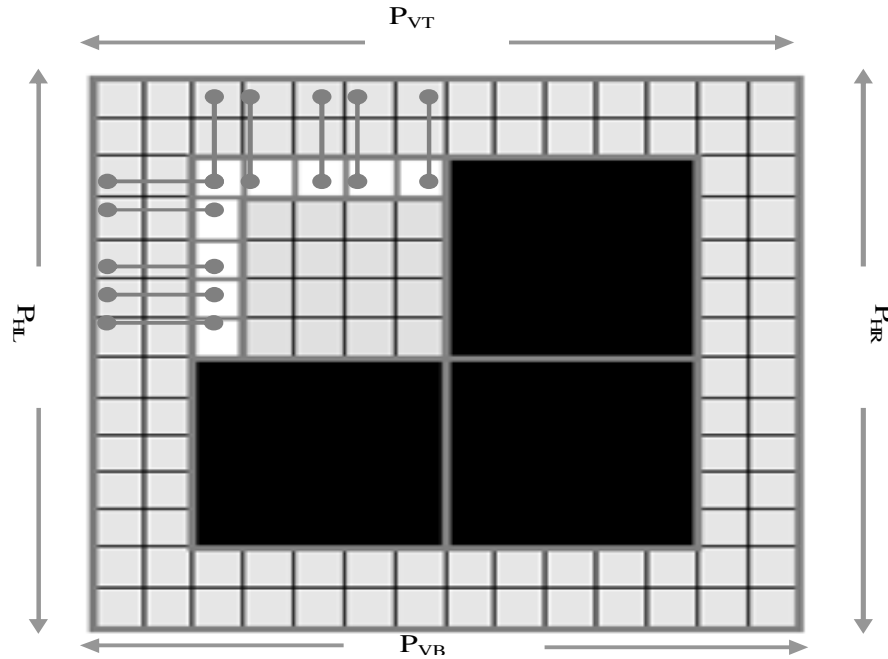


Figure 1. The proposed error concealment innovator.

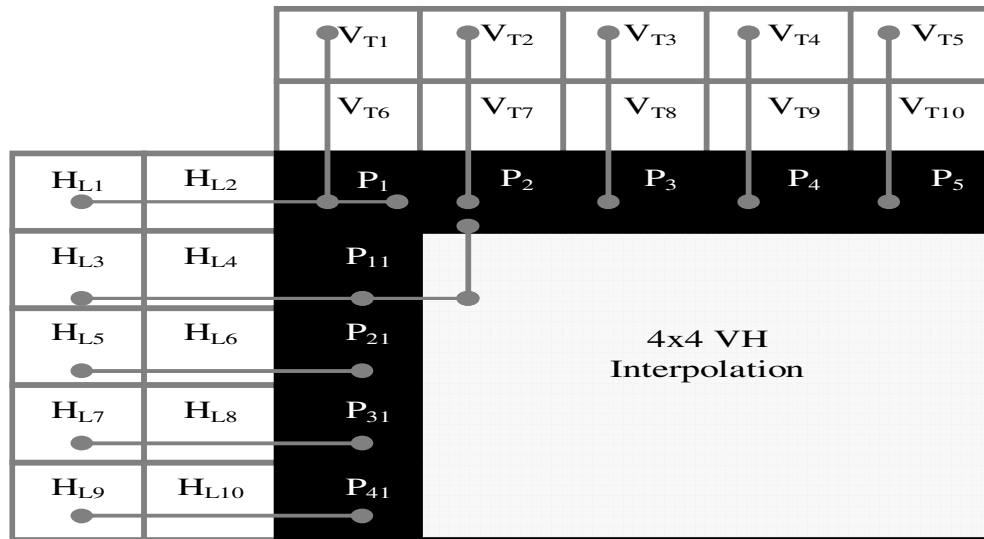
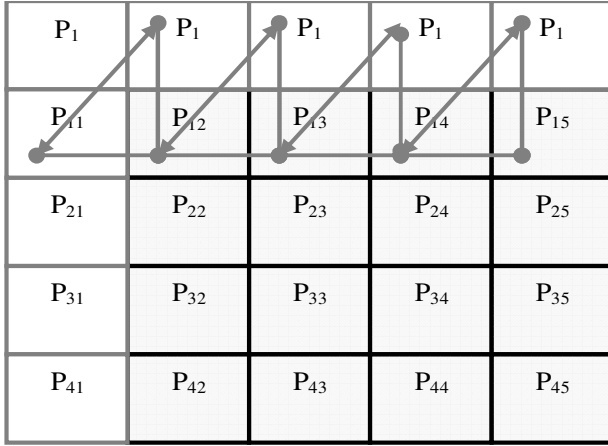


Figure 2. The first-step for the vertical and horizontal interpolation for border pixels.

that artifacts (for example blurring, blocking, etc.) were degraded to the minimal extent. In the meantime, pixels of the border: left, right, top, and bottom was estimated either with horizontal or vertical interpolation analysis, respectively. While, the remaining pixels of each quarter were simultaneously guessed with both vertical and horizontal interpolation analysis. The proposed technique had the capability to successfully reconstruct the image details for both low and high sub-band frequencies. At first, we needed to decide whether the missing blocks occurred in smooth or non-smooth areas. In the case of smooth regions, the loss coefficients are estimated by interpolating these coefficients with undamaged

adjacent pixels. While, for non-smooth regions (for example, edge components), the damaged blocks were portioned into sub-damaged blocks, for the purpose of exploiting all the border pixels, this leads to a significant reduction in the effects of each of the blocking and blurring.

Figure 2, shows the first step of our proposed method, for estimating the border missing pixels. In this context, the guessed results to the four quarters were carried out by apportioning those quarters to two matrices: 1) the border matrix, and 2) the inner matrix. Figure 3 shows the second step of our proposed method used to conceal the remaining coefficients (for example, inner



**Figure 3.** The second-step for interpolating the remaining inner matrix cells.

matrix). Here, each element from this matrix was estimated with two fresh adjacent border pixels, for example, one from vertical border pixels and one from horizontal border pixels respectively. Let us now consider the missing block. Let  $P_S$ , ( $S = 10 \times 10$ ),  $P_S$ , be the pixel size. In this case, the cell's number of each quarter is  $5 \times 5$  pixels. Here, only  $P_1(i, j)$  was interpolated either by the two vertical adjacent pixels  $P_{VT1}(i, j), P_{VT6}(i, j)$  or by the two horizontal adjacent pixels  $P_{HL1}(i, j), P_{HL2}(i, j)$  as shown in Equation 1 and 2:

$$P_1(i, j) = w_1 \times P_{VT1}(i, j) + w_2 \times P_{VT6}(i, j) \quad (1)$$

$$P_1(i, j) = w_1 \times P_{HL1}(i, j) + w_2 \times P_{HL2}(i, j) \quad (2)$$

Where,  $w_1$  &  $w_2$  are scalar parameters.

Whereas, remaining four border pixels located at the top.  $P_2, P_3, P_4$ , and  $P_5$  were interpolated by the two vertical adjacent pixels. Similarly, remaining four border pixels located at the left  $P_{11}, P_{21}, P_{31}$ , and  $P_{41}$  were interpolated by the two horizontal adjacent pixels, as shown in Equation 3 and 4:

$$P_2(i, j) = w_1 \times P_{VT2}(i, j) + w_2 \times P_{VT7}(i, j) \quad (3)$$

$$P_{11}(i, j) = w_1 \times P_{HL3}(i, j) + w_2 \times P_{HL4}(i, j) \quad (4)$$

Finally, to guess the remaining cells for the  $4 \times 4$  inner sub-matrix requires us for exploiting the estimated results of the border cells at the top and the left respectively. Here,  $P_{12}(i, j)$  can be estimated as shown in the following formula.

$$P_{12}(i, j) = w_1 \times P_2(i, j) + w_2 \times P_{11}(i, j) \quad (5)$$

Let us now consider that the pixel  $P_{12}$  is the missing pixel. The mean absolute difference (MAD) can be expressed as:

$$MAD(S_S) = \sum_{i=0}^{M-1} I_{0,i}^{P_1} - I_{M-1,i+S_S}^{P_2,P_1} \quad (6)$$

Where,  $S_S$  is a search vector that is from  $-M$  to  $M$  if the block size is to be  $(M \times M)$ . Accordingly, we can evaluate the best match (BMA) with respect to the minimum (MAD) value as shown:

$$BMA = Min.(MAD(S_S)), \quad S_S, \quad \text{from } -M \text{ to } M \quad (7)$$

To ensure finding an appropriate vector to match the blocks  $p_1$ , and the blocks  $p_2, p_{11}$  in the boundary after comparing  $2M$   $MAD_S$ , the vector can be exploited to give direction to the edge for the corrupted block. If, the direction is between  $0^\circ \rightarrow 45^\circ$ , the perfect match should be appointed between the blocks  $p_2$ , and  $p_3$ . In other cases, if the edge direction is located between  $90^\circ$  and  $135^\circ$ , the perfect match should be appointed between  $p_1$  and  $p_2$ . Furthermore, if the guessed outcome of the perfect match value is less than the threshold, this emphasizes that there is a meaningful edge or fleecy patch among adjacent blocks. Meanwhile, the interpolation process was achieved between the lost pixels and the undamaged adjacent pixels along the direction of the perfect vector. This can be assessed by using the following format:

$$\hat{I}_{m1,n1}^1 = I_{M-1,i}^{P_1,P_2,P_3} \times \frac{D_2}{N} + I_{0,k}^{P_{22}} \times \frac{D_1}{N} \quad (8)$$

Where,  $N$  is the maximum number of pixels to be interpolated with the required direction.  $D_1$  and  $D_2$  are the distances between pixels to be interpolated in the process of the best boundary matching.

### Smooth error concealment

Figure 4 illustrated the guessed results of the proposed technique, which were very convincing in terms of visual quality to the reconstructed image, through enlarging of the concealing region. Although, the simulation has been carried out with images that have high resolution, we have seen that the area of concealment does not show any significant effects whatsoever. Considering, the procedural steps for concealing the first quarter was carried out in smooth regions. Let us view a similar example but now with image snapshot of computed tomography (CT). Figure 5 illustrates the procedural steps of our proposed technique for concealing patches that occurred within smooth regions. Further, the concealment included only the smooth part of the corrupted patch in the center of the snapshot.

### Edge detection

An edge is a hop in intensity, or a curve that tracks the transition of rapid change in image intensities. There are many methods to perform edge detection, most of these methods can be classified into two categories: 1) gradient, and 2) Laplacian. In the gradient

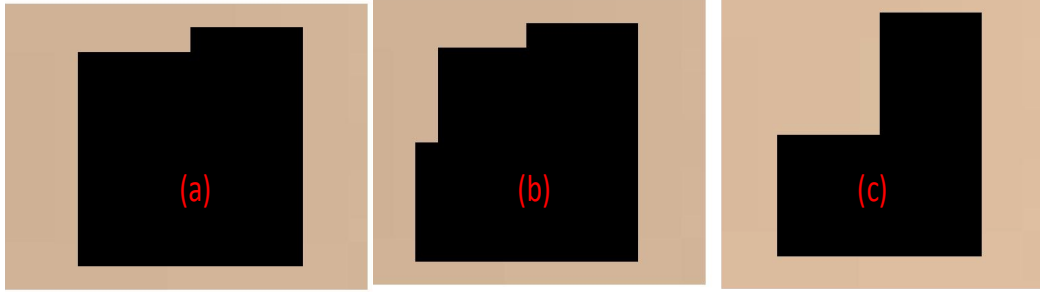


**Figure 4.** Steps of concealment to the first quarter of image, in which the damaged patch occurred within a smooth area; (a) top border; (b) left border, and (c) 4x4 inner matrix cells.

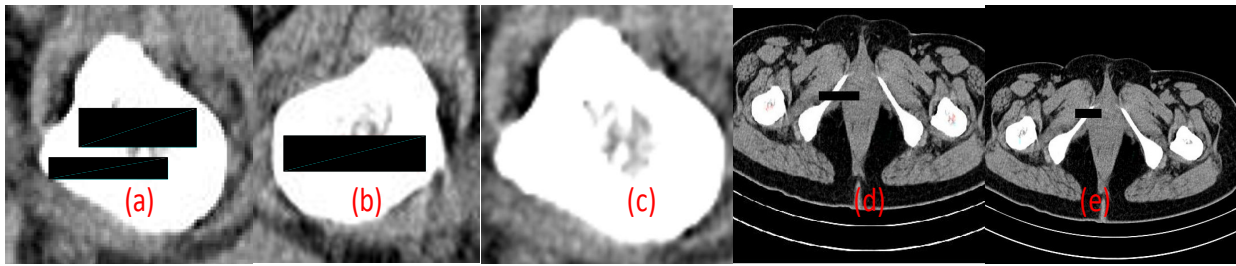


**Figure 5.** The procedural steps of our proposed technique for concealing the damaged patches of a CT image; (a) damaged area; (b) concealing of the first patch; (c) concealed area; (d) concealing of part of a smooth area from the left side; (e) concealing of part of a smooth area from the right side.

method, the edges were detected by viewing for both maximum and minimum magnitude in the first derivative of the image, whereas, in a Laplacian method these edges were detected by inspection for zero-crossings in the second derivative of the image. Here is another method that shows how to detect the edges, whereby the trend was in the correct format and on the uses of wavelet transformations. Here and limitedly, decomposition of the Haar-wavelet for two-dimensional images produced substantially edges maps from vertical, horizontal, and diagonal analysis.

Technically, edge detection operator, is a discrete differentiation operator used to calculate the intensity image gradients approximations. Typical image edges had been calculated in two different ways: 1) by finding the best parameters to be used with a set of test images, and 2) by adapting of these parameters for each test image. For clarity, the most beefy edge detection method, in which the edge was an already true edge was the canny method. The canny edge detector was used to optimize so many edge detectors. Accordingly, it is used for smoothing the images to remove the noise as well as, finding image gradients to display patches with the high spatial derivatives. In this paper, each gradients magnitude and gradients orientation were expressed in terms of the following directional derivatives:  $\partial_v I(i, j)$  and  $\partial_h I(i, j)$ . The gradients' magnitude was calculated as:

$$|\nabla I(i, j)| = \sqrt{(\partial_v I(i, j))^2 + (\partial_h I(i, j))^2} \quad (9)$$

Where,  $I(i, j)$  is a continuous image,  $i$  and  $j$  are the row, and column coordinates respectively.

And the gradients' orientation was given by the following format:

$$\angle \nabla I(i, j) = \text{ArcTan}(\partial_h I(i, j) / \partial_v I(i, j)) \quad (10)$$

The magnitude of the edge gradient identified by the Local maximum in  $I(i, j)$ . In the case where the first derivative had given the maximum magnitude, the second derivative is zero. For this reason, an alternative edge-direction strategy to locate zeros of the second derivatives of  $I(i, j)$  was required, and differential operator called zero-crossing edge detectors was the Laplacian:

$$\Delta I(i, j) = \partial_{(v_2)} I(i, j) + \partial_{(h_2)} I(i, j) \quad (11)$$

Practically, finite difference approximations were achieved by using first-order directional derivatives, and were performed by a pair of masks, say and (for example Sobel, Roperitts, etc.) vertical and horizontal masks. Officially, these were linear-phase FIR filters used for attenuating the increase in pixel noise due to the differentiation. A convolution of the target image with these two masks gave two directional derivative images and respectively. Image gradients were traditionally calculated as follows:

$$\nabla = \sqrt{g_v^2 + g_h^2} \quad (12)$$

Or, alternatively using:

$$\nabla = |g_v| + |g_h| \quad (13)$$

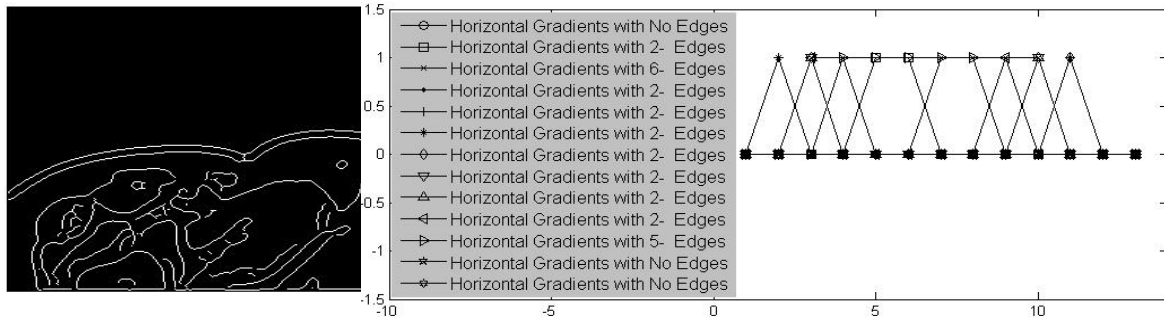


Figure 6. Canny edge detector, horizontal gradient, threshold = 0.15, sigma = 2, theta = -45 degree.

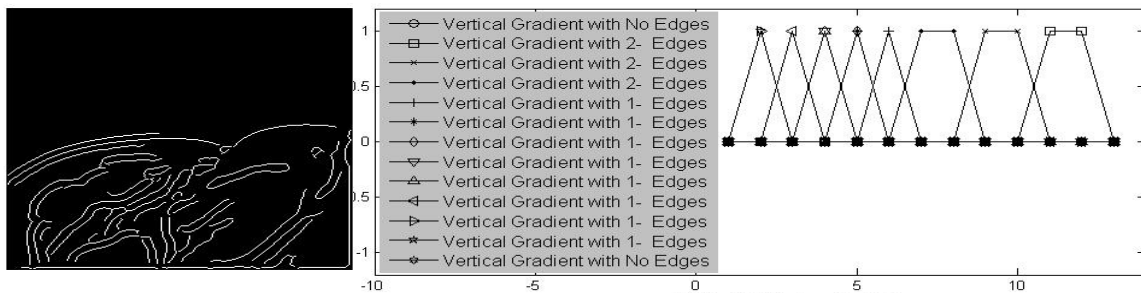


Figure 7. Canny edge detector, vertical gradient, threshold = 0.15, sigma = 2, theta = -45 degree.

Table 1. Canny edge detector, vertical and horizontal gradients, threshold = 0.15, sigma = 2, theta = -45 Deg.

0	0	0	0	0	0	0	0	0	0	0	0	0
0	0	0	0	1	1	0	0	0	0	1	1	0
0	0	1	1	0	0	1	1	1.4142	1.4142	0	0	0
0	1	0	0	0	0	1	1	0	0	1	0	0
0	1	0	0	0	1	0	0	0	0	1	0	0
0	1	0	0	1	0	0	0	0	0	1	0	0
0	0	1	0	1	0	0	0	0	0	1	0	0
0	0	1	1	0	0	0	0	0	1	0	0	0
0	0	1	1	0	0	0	0	0	1	0	0	0
0	0	1.4142	0	0	0	0	0	1	0	0	0	0
0	1	0	1	1	1	1	1	0	0	0	0	0
0	1	0	0	0	0	0	0	0	0	0	0	0
0	0	0	0	0	0	0	0	0	0	0	0	0

0 – No Edge, 1 – Initial Edge, 1.4142 – Edge.

Where, edge direction information is given by:

$$\alpha(i, j) = \tan^{-1}(G_h/G_v) \tag{14}$$

The spatial gradient,  $I(i, j) = [G_v^2 + G_h^2]^{1/2}$ , and edge direction  $\alpha(i, j) = \tan^{-1}(G_h/G_v)$ , were evaluated at each point. Figure 6 and 7 shows the simulated sketches to our proposed technique based on the Canny edge detector. Considering, the

simulation was achieved for the purpose of eliciting both vertical and horizontal image gradients by adopting the gradient direction with different angles. Table 1, explained that the ideals of the true edges, the pixels that have values of more than one.

#### Pixels-to-length conversion

Figure 8, shows a live CT image (512x512 pixels, 24-bit-depth), this image included on damaged patches were different in size and location, placed under the test for the purpose of concealing these

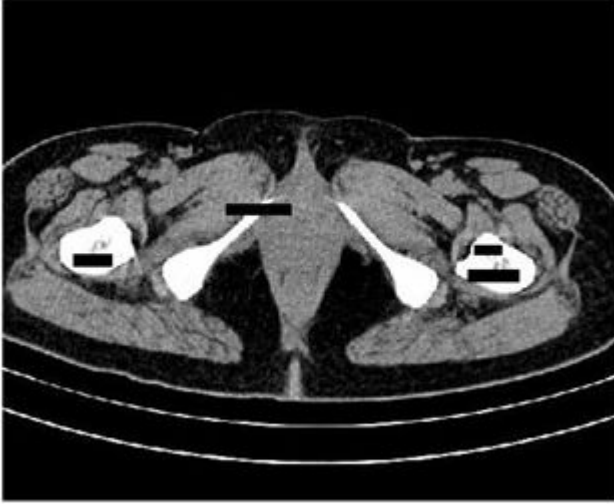


**Figure 8.** A CT image, 512x512 pixels, 24-bit-depth, contains on corrupted patches with various sizes and locations.

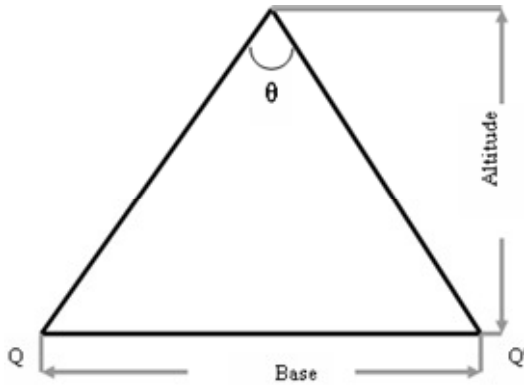


**Figure 9.** The block diagram of the similar triangle field of view (FOV).

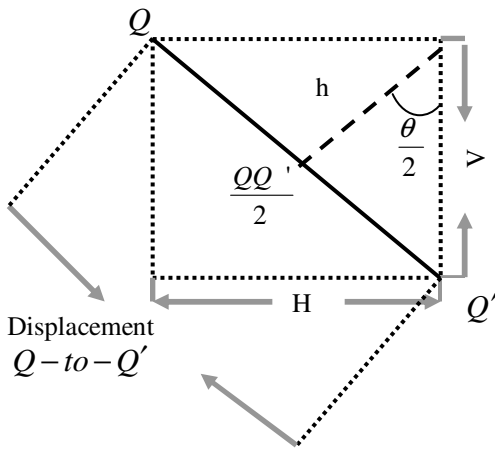


**Figure 10.** The block diagram of the image displacement.

patches. To compensate these damaged patches from non-damaged areas of the same image details of those patches, the edge components between the smooth and the non-smooth areas were separated. However, the damaged patches occurred in the smooth areas were successfully concealed by applying our proposed technique. Referring to Figure 8 again, we directly focused on the patch located at the middle of this snapshot, this is because both sides of this patch have been contained on the edges. Nevertheless, the vertical and horizontal image gradients were efficiently extracted from this patch. At first, we portioned this patch and then concealed their smooth parts. In the meantime, the concealed area has been enlarged, for the possibility of separation between the smooth and non-smooth areas in addition, to flexibility in dealing with artifacts. Here, some triangular forms emerged, which we found difficult to deal with, and specifically the manner to be followed to compensate these forms from un-damaged neighbors.

To fill-in these damaged triangles from areas that carry the same details, after the creation of similar triangles and in an effective manner. It, therefore, needed to propose an efficient innovator to actualize this purpose. The motivation behind the current implementation and the problem that we aim to solve, lies on how to convert the lengths of the base and height of those triangles from pixels-to-feet to calculate the areas of these truncated triangles for the purpose of compensation.

Geometric computation of the height of these triangles was calculated by using the geometric algebra, and the angle " $\theta$ " was utilized to bring on the width of the field of view (FOV). Figure 9 explained the basic concepts to calculate both the height and base of the triangle, after halving the angle  $\theta$ . Therefore, the length of the base should be converted from pixels to feet to obtain appropriate height. Let us now consider the time between successive truncated triangles  $dt$ , and also the velocity of portioning,  $V_{GPS}$ .

$$V_{GPS} = ft / second, \quad dt = second \quad (15)$$

The displacement in Figure 10 between and illustrated the shift in location between the image of two pixels for both vertical and horizontal directions. So, the displacement between and was given in the following format:

$$D_{Q \rightarrow Q'} = \sqrt{H^2 + V^2}, Pixels \quad (16)$$

Where  $H$  and  $V$  are the offsets between similar triangles for both horizontal and vertical directions respectively. For clarification, from the basic concepts of image processing, the velocity was calculated by the proportion of pixel displacement to the time required to truncate those triangles.

$$V_{PIX} = \frac{D_{Q \rightarrow Q'}}{dt}, Pixels / Sec \quad (17)$$

This velocity  $V_{PIX}$  indicates to the speed of the images in *pixels/second*. Since the length of the base of the image was in pixels, we needed to know how many in order to find the corresponding height in feet. The two velocities were combined to find the unit conversion:

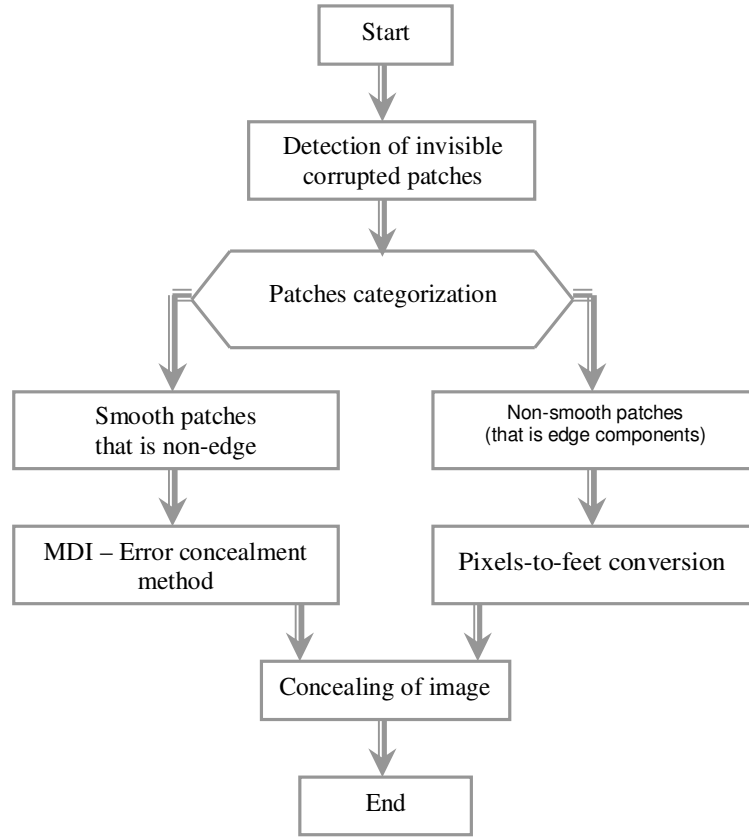


Figure 11. A flowchart of the proposed error concealment.

$$R = \frac{V_{GPS} (ft/sec)}{V_{PIX} (pixels/sec)} = ft / pixels \tag{17}$$

where  $R$  is the ratio between the displacement in feet to the displacement in *pixels* for a given triangle image.

In this context, and to find the height of the triangle image, we need to exploit the base length of the triangle image in *ft* to recover the size of the image in *pixels*. Since the length of the triangle base in *pixels* is already given by the viewing after enlarging the triangle image. Let us now assume the actual size of the base of the triangle image. Let  $A_P$ , be the size of the base of the triangle image and given as:

$$A_P = N.O.P, pixels \tag{18}$$

where,  $NOP$  is the number of pixels. In this case, the corresponding size of the base triangle image in *ft* is given as:

$$S = R \times A_P, \frac{ft}{pixels} \times pixels = ft \tag{19}$$

Meanwhile, the height of the truncated triangle is calculated as:

$$\tan \theta/2 = 0.5 \times QQ' / h \tag{20}$$

And,

$$h = \frac{0.5 \times QQ'}{\tan \theta/2} \tag{21}$$

Finally, we are able to successfully calculated the area of the estimated similar triangle by using "Hero's Formula" without applying  $\theta$  as:

$$Area = \sqrt{S \times (S - h) \times (S - QQ'/2) \times (S - V)} \tag{22}$$

Where  $S$ , is the semi-perimeter, and also given as:

$$Perimeter = QQ'/2 + V + h \tag{23}$$

And,

$$S = \frac{QQ'/2 + V + h}{2} \tag{24}$$

In order to conform with the validity of the performance efficiency of the proposed methods mentioned, a flowchart for concealing various patches based on the sort of method used in the concealment has been suggested. Figure 11 explained the proposed flowchart steps, in which patches of smooth and non-smooth are characterized. Further, classification of damaged

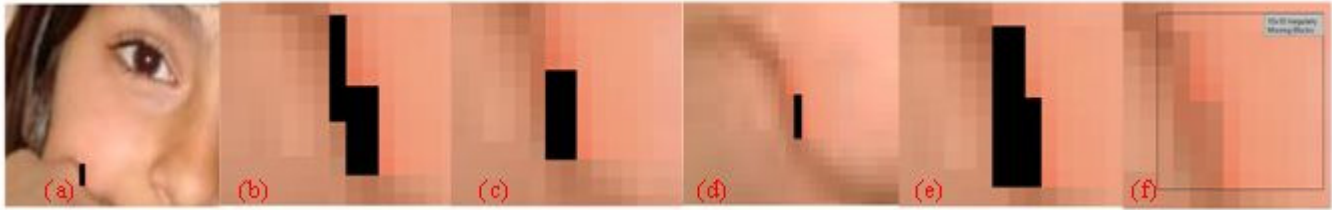


**Figure 12.** Safa. jpg (400x300x3 pixels, 24-Bit-depth) (a) Corrupted image (b) The first step to conceal the smooth regions (c) Second step to conceal (d) Edge region (e) The zooming-in for the edge region (f) Concealed image.



**Figure 13.** The Malaysian Working-woman image; (a) damaged image; (b) concealing of a smooth area; (c) concealing of a non-smooth area; (d) the concealed image.

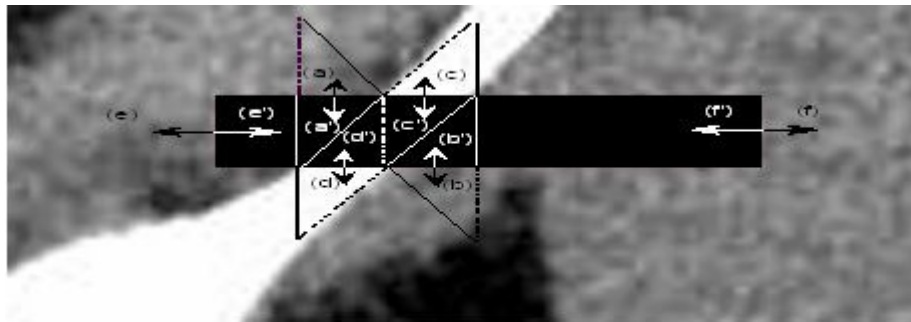


**Figure 14.** The compensatory truncating between triangles that contain on similar details from both damaged and undamaged regions.

patches within the locations of occurrence is considered as an effective indicator to extract the edges as well as flexibility in dealing with the effects that may appear during the process of filling-in of those patches.

## SIMULATION AND RESULTS

Results of the proposed algorithms for each of the error concealment based on the multi-directional interpolation, and algorithm for converting of pixels to the feet, which had been submitted to the chains: Safa image, snapshots from CT image, and the Malaysian working woman image. The main problem that faced the process of filling-in the damaged patches for these images were the edges. These edges, and specifically in the regular areas

created some small artifacts, for example, the impacts of each of the blurring and the blocking. For clarification, these influences were tackled to a limited extent, through the use of smooth candidates. Figures 12 and 13, showed the steps of concealment of chains of those images.

From these figures, we noted that the concealment for each of Safa and the Malaysian working woman were very close to the original images, except for somewhat of the impact of the blurring had been emerged. On the other hand, extracting the edges from image gradients introduced some unwanted deformations, which appeared after enlarging the filling-in areas. As a result, reflected negatively on the quality of visual images, which have been reconstructed. Figure 14 illustrated the proposed method for compensating the damaged

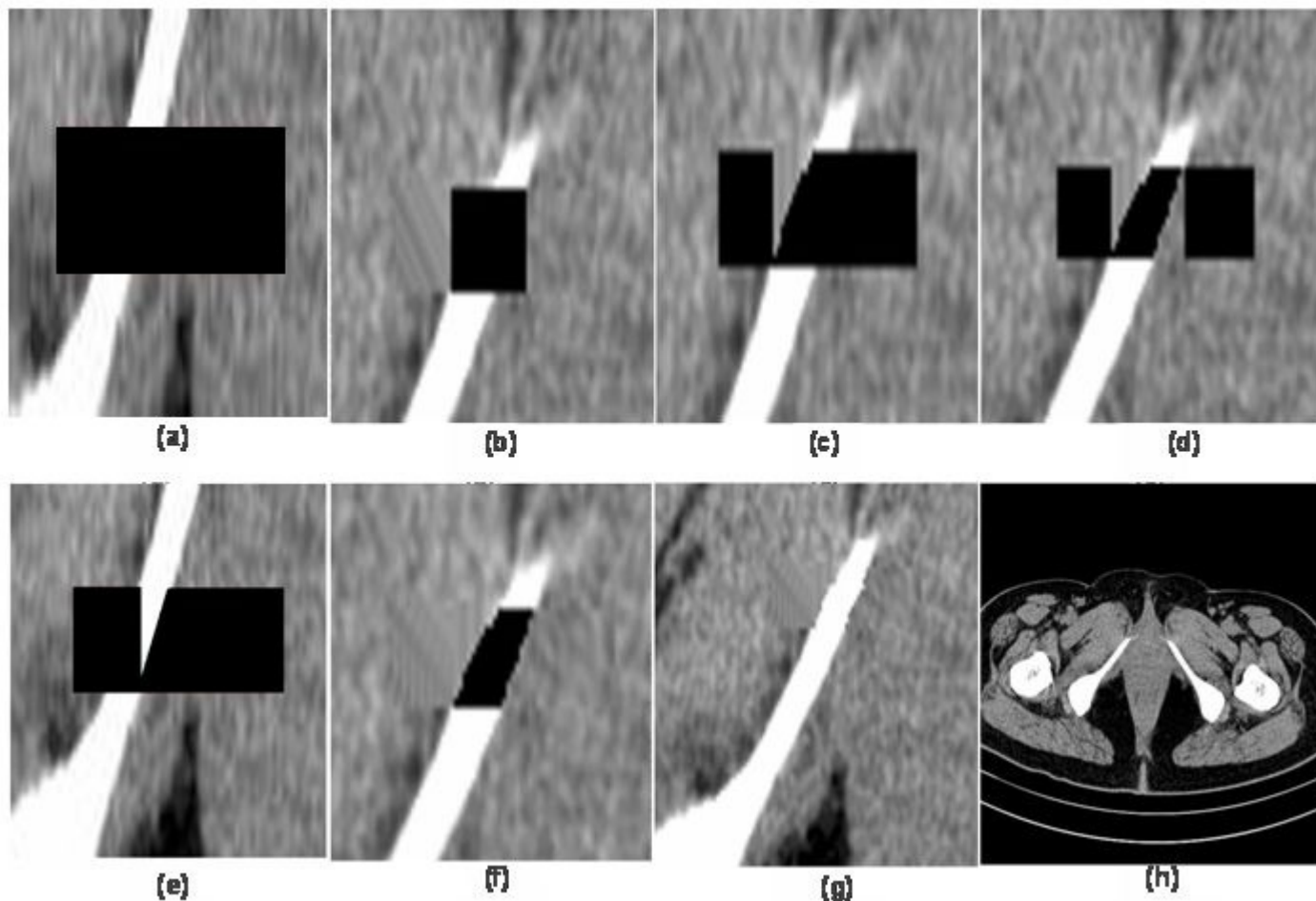


**Figure 15.** Results of the proposed second algorithm; (a) the edge region before truncating; (b) the region to be concealed; (c) concealing of a left-hand triangle; (d) concealing of a right-hand triangle; (e) concealing of middle-triangle; (f) smooth region (g) the concealed region; (h) the concealed image.

triangles within the smooth and non-smooth areas. Practically, the damaged patch at the middle were portioned into a set of homomorphous triangles, in which each triangle has been compensated with homomorphous image details within a similar non-damaged area. To eliminate the influences for both the blurring and the blocking, that may cause to loss the information at the high frequency areas, and also the imperfect loss after the reconstruction process. We have examined the performance of the process of the filling-in by forcing the proposed technique to a series of comprehensive tests. Here, the test included damaged patches, which were different in size and location and also within areas of smooth and non-smooth.

Figure 15 showed the procedural steps of our proposed algorithm, keeping in mind that we were carefully focused at the target area to examine the visual quality of the image, specifically on the portions that have been concealed. This was accomplished by enlarging the areas of filling-in of these images. Accordingly, the

enlarging image in Figure 15 (g) showed the area of concealment. The region does not contain any impacts.

## DISCUSSION

We have demonstrated that the proposed technique and during the discussion of the results were convincing and efficient. So we were forced to re-simulation with more than one snapshot to prove the efficiency of the proposed technique. In this paper, we adopted a simulation of seventeen live snapshots. Tables 2 and 3, described the simulation results of seventeen medical snapshots with unremitting motions. In this simulation, the results showed the total number of pixels that have occurred in error. Often, the results were very close to the desired values, as shown in the simulation graphs. To implement the results obtained from the above tables, Figure 16 explained the relationship between the total number of pixels of the tested patch and the magnitude of the pixels. At

**Table 2.** A CT-image (512x512x3 pixels, 24- Bit-Depth) 24- Bit-Depth, 11x31 missing pixels, seventeen snapshots with slow unremitting motions.

No. of snapshot	No. of pixels in error	Error value
Image-1	10	0.0432
Image-2	12	0.0519
Image-3	7	0.0303
Image-4	6	0.0259
Image-5	6	0.0259
Image-6	2	0.0086
Image-7	4	0.0173
Image-8	5	0.0216
Image-9	8	0.0346
Image-10	6	0.0259
Image-11	9	0.0389
Image-12	11	0.0476
Image-13	10	0.0432
Image-14	12	0.0519
Image-15	18	0.0779
Image-16	23	0.0995
Image-17	23	0.0995

**Table 3.** A CT-image (512x512x3 pixels) 11x21 missing pixels, seventeen snapshots with slow unremitting motions.

No. of snapshot	No. of pixels in error	Error value
Image-1	0	0
Image-2	0	0
Image-3	1	0.0001
Image-4	0	0
Image-5	1	0.0001
Image-6	2	0.0058
Image-7	5	0.0146
Image-8	5	0.0146
Image-9	6	0.0175
Image-10	13	0.0381
Image-11	11	0.0322
Image-12	11	0.0322
Image-13	9	0.0263
Image-14	17	0.0498
Image-15	23	0.0674
Image-16	15	0.0439
Image-17	44	0.129

the same time, the sketches showed percentages of pixels occurred in error. In most cases, the algorithm gave good and convincing results.

## Conclusions

In this paper, two algorithms were proposed, the first algorithm was a low complexity error concealment based on

a multi-directional interpolation, while the second was used to convert pixels to feet. In the MDI, the damaged blocks were efficiently recovered whether located in smooth or non-smooth areas. In the case of smooth regions, the loss coefficients were estimated by interpolating these coefficients with the undamaged neighbors. While, for non-smooth regions (for example, edge components), these blocks were portioned into at least four quarters, with the intention to exploit all border pixels. In the

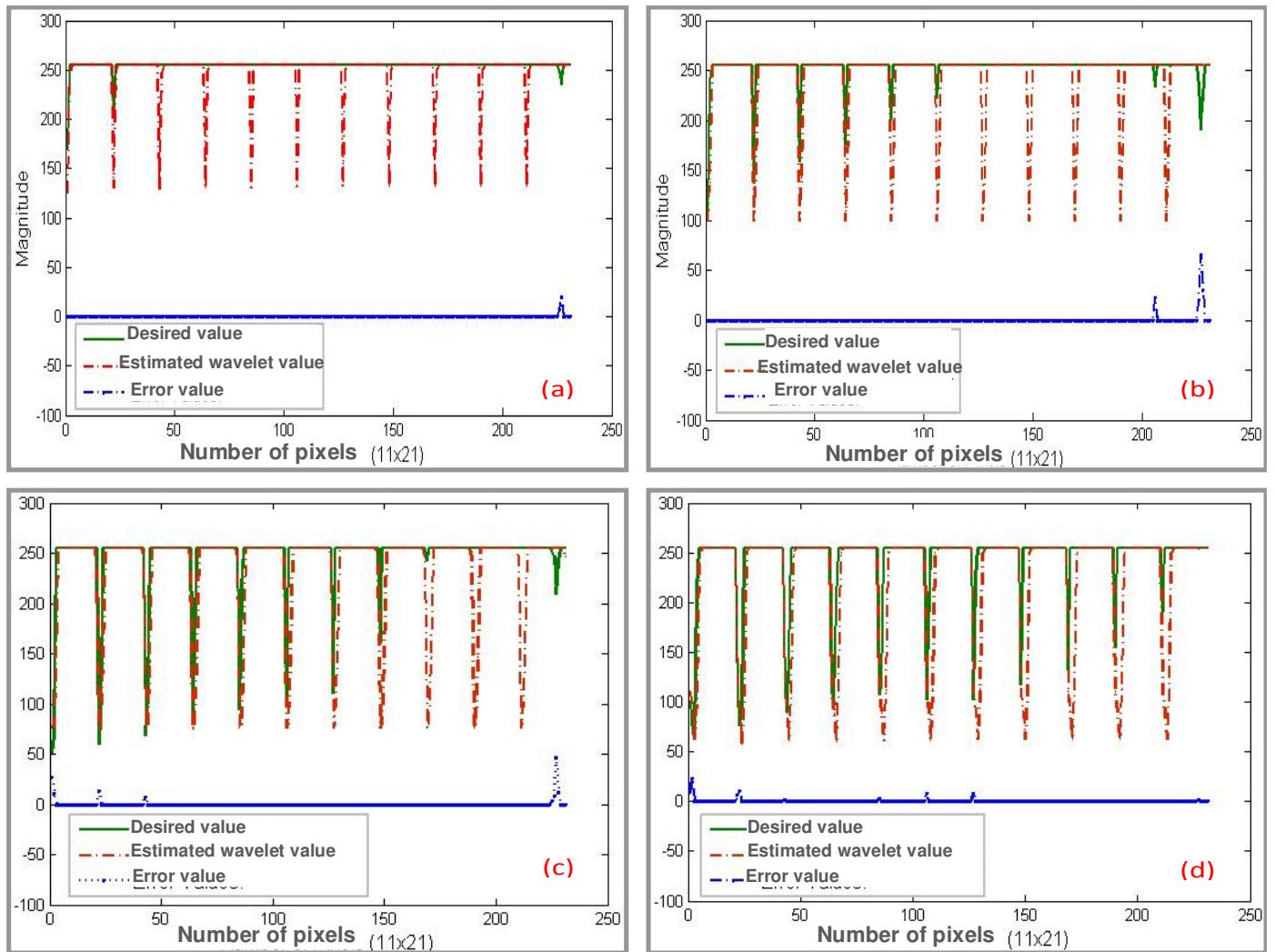


**Figure 16.** The relationship between the total number (1:231) for the matrix pixels (11×21) and the magnitude of each pixel; (a) two pixels in the error; (b) four pixels in the error; (c) eight pixels in the error; (d) twelve pixels in the error, while, rates of error were (0.0086,0.0173,0.0346,0.0519), respectively.

meantime, pixels of the border left and right were estimated with horizontal interpolation, and pixels of the border top, and bottom were estimated with vertical interpolation. The remaining pixels of each quarter were guessed with vertical and horizontal interpolation simultaneously.

The lengths of each base and height of the triangles, which was truncated from damaged and undamaged patches were converted from pixels to the feet. The motivation behind this work is to overcome the effects of each blurriness and blockiness specifically, with areas that contain the edges. Experimental results were very close to the desired values as shown in the simulated graphs. The likelihood of our proposed algorithm for error concealment in various image regions was a distinct and as summarized in the Tables 1 and 2, respectively.

## ACKNOWLEDGEMENT

This work was supported by the Department of Communications and Computer Engineering, University Putra Malaysia (UPM). The authors would, firstly, like to thank God, and all the UPM staff and friends who gave us help related to this work.

## REFERENCES

- Al-Mualla M, Canagarajah N, Bull DR (1999). Temporal Error Concealment Using Motion Field Interpolation. *Electron. Lett.*, 35(3): 215-217.
- Alter F, Durand S, Froment J (2004). DCT-based compressed images with weighted total variation. *IEEE Int. Con. Acoustics, Speech, and Signal Process.*, 3: 221-224.

- Bajic I (2006). Adaptive MAP Error Concealment For Dispersively Packetized Wavelet-Coded Images. *IEEE Trans. Image Process.*, 15(5): 1226-1235.
- Chen M, Chen C, Chi M (2005). Temporal Error Concealment Algorithm By Recursive Block-Matching Principle. *IEEE Trans. Circuits Syst. Video Technol.*, 15(11): 1385-1393.
- Chen Y, Hu Y, Au OC, Li H, Chen CW (2008). Video Error Concealment Using Spatio-Temporal Boundary Matching and Partial Differential Equation. *IEEE Trans. Multimed.*, 10(1): 2-15.
- Chi M, Chen M, Liu J, Hsu C (2005). High Performance Error Concealment Algorithm by Motion Vector Refinement For MPEG-4 Video. *Int. Conf. Circuits Syst.*, 3: 2895-2898.
- Chung KL, Huang TH, Liao PH (2007). Efficient Hybrid Error Concealment Algorithm Based on Adaptive Estimation Scheme. *J. Vis. Commun. Image Rep.* 18(4): 331-340.
- Feng J, Lo K, Mehropour H, Karbowski AE (1997). Error Concealment for MPEG Video Transmissions. *IEEE Trans. Consum. Electron.*, 43(2): 183-187.
- Fu CM, Hwang WL, Huang CL (2005). Efficient Post-Compression Error-Resilient 3D-Scalable Video Transmission For Packet Erasure Channels. *IEEE International Conference on Acoustics, Speech, and Signal Processing (ICASSP'05)*. 2: 305-308.
- Gothandaraman A, Whitaker RT, Gregor J (2001). Total variation for the removal of blocking effects in DCT based encoding. *IEEE Int. Con. Image Process.*, 2: 455-458.
- Guo Y, Chen Y, Wang YK, Li H, Hannuksela MM, Gabbouj M (2009). Error Resilient Coding and Error Concealment in Scalable Video Coding. *IEEE Trans. Circuits Syst. Video Technol.*, 19(6): 781-795.
- Hemami SS, Meng THY (1995). Transform Coded Image Reconstruction Exploiting Inter-block Correlation. *IEEE Trans. Image Processing.*, 4(7): 1023-1027.
- Hsia SC (2004). An Edge-Oriented Spatial Interpolation for Consecutive Block Error Concealment. *IEEE Signal Process. Lett.*, 11(6): 577-580.
- Kang LW, Leou JJ (2006). Two Error Resilient Coding Schemes for Wavelet-Based Image Transmission Based on Data Embedding and Genetic Algorithms. *J. Vis. Commun. Image Rep.*, 17(6): 1127-1144.
- Kaup A, Meisinger K, Aach T (2005). Frequency selective signal extrapolation with applications to error concealment in image communication. *AEU-Int. J. Electron. Commun.*, 59(3): 147-156.
- Kim BJ, Xiong Z, Pearlman WA (2000). Low bit-rate scalable video coding with 3-d set partitioning in hierarchical trees (3-D SPIHT). *IEEE Trans. Circuits Syst. Video Technol.*, 10(8): 1374-1387.
- Kim J, Mersereau RM, Altunbasak Y (2004). A Multiple-Substream Unequal Error-Protection and Error Concealment Algorithm For Spihtcoded Video Bitstreams. *IEEE Trans. Image Process.*, 13(12): 1547-1553.
- Kung WY, Kim CS, Kuo C.-CJ (2006). Spatial and Temporal Error Concealment Techniques for Video Transmission Over Noisy Channels. *IEEE Trans. Circuits Syst. Video Technol.*, 16(7): 789-803.
- Lee YC, Altunbasak Y, Mersereau R (2001). A Temporal Error Concealment Method for MPEG Coded Video Using A Multi-Frame Boundary Matching Algorithm. *IEEE Int. Conf. Image Process.*, 1: 990-993.
- Lee YS, Ong KK, Lee CY (2003). Error-Resilient Image Coding (ERIC) With Smart-IDCT Error Concealment Technique for Wireless Multimedia Transmission. *IEEE Trans. Circuits Syst. Video Technol.*, 13(2): 176-181.
- Li X, Orchard M (2002). Novel Sequential Error-Concealment Techniques Using Orientation Adaptive Interpolation. *IEEE Trans. Circuits Syst. Video Technol.*, 12(10): 857-864.
- Ma M, Au OC, Guo L, Chan SHG, Wong PHW (2008). Error Concealment for Frame Losses in MDC. *IEEE Trans. Multimed.*, 10(8): 1638-1647.
- Nafaa A, Taleb T, Murphy L (2008). Forward Error Correction Strategies For Media Streaming Over Wireless Networks. *IEEE Commun. Mag.*, 46(1): 72-79.
- Park CS, Nam HM, Jung SW, Baek SJ, Ko SJ (2009). Practical Error Concealment Strategy for Video Streaming Adopting Scalable Video Coding. *IEEE Trans. Consum. Electron.*, 55(3): 1606-1613.
- Persson D, Eriksson T (2009). Mixture Model- and Least Squares-Based Packet Video Error Concealment. *IEEE Trans. Image Process.*, 18(5): 1048-1054.
- Persson D, Eriksson T, Hedelin P (2008). Packet Video Error Concealment With Gaussian Mixture Models. *IEEE Trans. Image Process.*, 17(2): 145-154.
- Qian X, Liu G, Wang H (2009). Recovering Connected Error Region Based on Adaptive Error Concealment Order Determination. *IEEE Trans. Multimed.*, 11(4): 683-695.
- Rombaut J, Pižurica A, Philips W (2009). Passive Error Concealment for Wavelet-Coded I-Frames With an Inhomogeneous Gauss-Markov Random Field Model. *IEEE Trans. Image Process.*, 18(4): 783-796.
- Rongfu Z, Yuanhua Z, Xiaodong H (2004). Content-Adaptive Spatial Error Concealment for Video Communication. *IEEE Trans. Consum. Electron.*, 50(1): 335-341.
- Shin JH, Jung JH, Paik JK (1999). Spatial Interpolation of Image Sequences Using Truncated Projections Onto Convex Sets. *IEICE Trans. Fund.*, E82-A(6): 887-892.
- Simchony T, Chellapa R, Lichtenstein Z (1990). Relaxation For MAP Estimation of Gray Level Images Corrupted By Multiplicative Noise. *IEEE Trans. Inf. Theory*, 36(3): 608-613.
- Suh J, Ho Y (2004). Error concealment techniques for digital TV. *IEEE Trans. Broadcasting*, 48(4): 299-306.
- Tsekeridou S, Pitas I (2000). MPEG-2 Error Concealment Based on Block-Matching Principles. *IEEE Trans. Circuits Syst. Video Technol.*, 10(4): 646-658.
- Wang J, Zhu S, Gong Y (2010). Resolution Enhancement Based on Learning The Sparse Association of Image Patches. *Patt. Recog. Lett.*, 31(1): 1-10.
- Wang Y, Reibman A, Lin S (2005). Multiple Description Coding For Video Delivery. *IEEE J.*, 93(1): 57-70.
- Wang Y, Wenger S, Wen J, Katsaggelos AK (2000). Review of Error Resilient Coding Techniques For Real-Time Video Communications. *IEEE on Signal Process. Mag.*, 17(4): 61-82.
- Wang Z, Yu Y, Zhang D (1998). Best Neighborhood Matching: An Information Loss Restoration Technique for Block-Based Image Coding Systems. *IEEE Trans. Image Processing.*, 7(7): 1056-1061.
- Yang S, Hu YH (1997). Coding artifacts removal using biased anisotropic diffusion. *IEEE Int. Conf. Image Process.*, 2: 346-349.
- Zeng W, Liu B (1999). Geometric Structured Based Error Concealment With Novel Applications in Block-Based Low-Bit-Rate Coding. *IEEE Trans. Circuits. Syst. Video Technol.*, 9(4): 648-665.